

# Facile Synthesis and Characterization of Pyrolusite, $\beta$ - $\text{MnO}_2$ , Nano Crystal with Magnetic Studies

J.S Sherin  
Department of Physics,  
Karunya University,  
Coimbatore 641114,  
India.

J.K. Thomas  
Department of Physics,  
Electronic Materials Research  
Laboratory, Mar Ivanios  
college, University of Kerala,  
Thiruvananthapuram 695015,  
Kerala, India

Shiney Manoj  
Department of Physics,  
Christian College  
Kattakada, University of  
Kerala,  
Thiruvananthapuram  
695572, Kerala, India

**Abstract:**  $\text{MnO}_2$  nanoparticles have been synthesized by a simple combustion method using  $\text{MnSO}_4 \cdot 4\text{H}_2\text{O}$ . The crystalline phase, morphology, optical property and magnetic property of the as prepared nanoparticle were characterized using XRD, FT-IR, FT-Raman, SEM, UV-Vis, PL and VSM respectively. Structural studies by XRD indicate that the synthesized material as tetragonal rutile crystal structure. FT-IR and FT-Raman analysis revealed the stretching vibrations of metal ions in tetrahedral co-ordination confirming the crystal structure. The PL and UV analysis having an emission band at 390 nm, showed a prominent blue peak at 453 nm as well as a green emission lines at 553 nm with band gap energy of 3.2eV. Magnetic measurements indicate that the Néel temperature of the  $\beta$ - $\text{MnO}_2$  structures is 92.5K for  $H_c = 100$  Oe which showed antiferromagnetic behaviour.

**Keywords:** Nanostructures; Chemical synthesis; X-ray diffraction; Magnetic properties.

## 1. INTRODUCTION

Nanostructured manganese dioxides and their derivative compounds have special attention owing to their potential application in photonics, catalysis, magnetic fluids and magnetic resonance imaging [1] Manganese dioxide ( $\beta$ - $\text{MnO}_2$ , Pyrolusite) is a magnetic transition metal consisting of  $\text{Mn}^{4+}$  cation and  $\text{O}_2^{2-}$  anion. The different crystallographic forms are responsible for their electrochemical and magnetic properties [2]. The stable isomorph of  $\text{MnO}_2$  is the mineral pyrolusite,  $\beta$ - $\text{MnO}_2$ . It is a tetragonal rutile type ( $P4_2/mnm$  (136) space group), in which the basic motif is an infinite chain of  $\text{MnO}_6$  octahedra sharing two edges. However, the bridging Mn-O distances within a chain are shorter than the apical Mn-O distance within the basal planes. The structure consists of strings of  $\text{MnO}_6$  octahedra and empty channels corresponding to a width of (1 $\times$ 1) octahedron [3]. However there are only few reports on the synthesis of Mn based nanoparticles and relating its magnetic characteristics with particle size [4].

Various approaches have been used to fabricate manganese dioxide, such as self-reacting microemulsion [5], precipitation [6], room-temperature solid reaction [7], sonochemical [8], hydrothermal methods [9] and combustion synthesis [10]. The combustion synthesis method is a powerful approach for synthesizing various forms of manganese oxides and affords advantageous features including the use of mild synthesis conditions such as pH and temperature, and a wide range of precursors that can be used. Henceforth, the controlled synthesis of manganese dioxide nanostructures with favourable surface morphology, phase structure, crystallinity, and high reproducibility remains a considerable challenge [11].

This paper reports the controlled synthesis of  $\text{MnO}_2$  nanostructures via combustion without using any physical template and addition of any surfactant. The structural, morphological, vibrational, optical characteristics and field dependent magnetization study of the synthesized material is also presented.

## 2. EXPERIMENTAL ANALYSIS

### 2.1 Synthesis of nanopowders

A modified auto igniting solution combustion technique, was used for the synthesis of  $\text{MnO}_2$  nanoparticles. Aqueous solution containing ions of Mn was prepared by dissolving stoichiometric amount of high purity  $\text{MnSO}_4 \cdot 4\text{H}_2\text{O}$  in double distilled water in a beaker. Citric acid was added to the solution containing Mn ions. Amount of citric acid was calculated based on total valence of the oxidising and the reducing agents for maximum release of energy during combustion. Oxidant/Fuel ratio of the system was adjusted till the ratio was at unity. The solution containing the precursor mixture was heated using a hot plate in a ventilated fume hood. The solution boils on heating and undergoes dehydration accompanied by foam. The foam then ignites by itself on persistent heating giving voluminous and fluffy blackish grey product on combustion. The combustion product was calcinated at about 750  $^\circ\text{C}$  for 1 hour. The final powder was collected for characterization and characterised as single-phase nanocrystals of  $\text{MnO}_2$ .

### 2.2 Characterization.

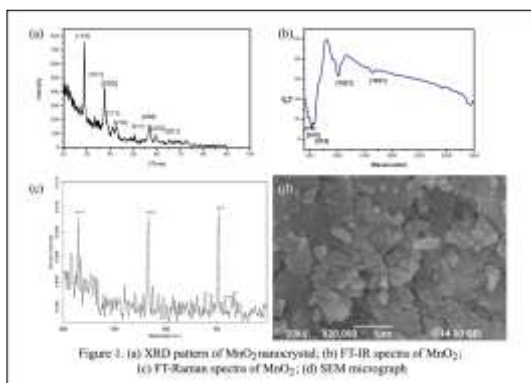
The as-prepared nanopowders were characterized by XRD (XPRT – PRO) diffractometer using  $\text{Cu } k_\alpha$  radiation source in the region 20 $^\circ$ –90 $^\circ$ . Fourier transform infrared (FT-IR) spectra were recorded using a Thermo Nicolet, Avatar 370 FT-IR Infrared spectrometer. Fourier transform Raman spectra were recorded using Bruker RFS FT-Raman Spectrometer. SEM picture was recorded using a JEOL/EOJSM – 6390 instrument. The UV-Vis absorption spectra were recorded for the as prepared samples using a Shimadzu UV-Vis 2400 PC spectrophotometer. The PL spectra were recorded using Shimadzu RF 5301PC spectrophotometer in the range 300 – 550nm. VSM measurements were performed using a Quantum Design Vibrating sample magnetometer. The sample was measured between 1KOe – 15KOe at 15K. ZFC and FC measurements

were carried out at 100 Oe and the blocking temperature was determined.

### 3. RESULTS AND DISCUSSION

Figure 1a shows the XRD pattern of the synthesised material where all the diffraction peaks in the pattern can be indexed to tetragonal  $\beta$ -MnO<sub>2</sub> (JCPDS card No 24-0735) with space group P4<sub>2</sub>/mnm (136) in primitive lattice. The diffraction pattern exhibits characteristic peaks having tetragonal phase of  $\beta$ -MnO<sub>2</sub> with lattice constants  $a = 4.3743 \text{ \AA}$  and  $c = 2.8573 \text{ \AA}$ , which are in good agreement with the reported data ( $a = 4.3999 \text{ \AA}$  and  $c = 2.8739 \text{ \AA}$ ). The broad diffraction peaks maybe due to the nanosize effects on the products. The calculated average crystallite size was 23.05nm. The XRD pattern showed that they are predominantly composed of tetragonal lattice structure.

Figure 1b shows FT-IR spectra of as-prepared  $\beta$ -MnO<sub>2</sub> nanoparticles without any thermal treatment displays three significant absorption bands in the range of 400 – 700 cm<sup>-1</sup>, where stretching and bending vibrations of [MnO]<sub>n</sub> units are showing up and are in good agreement with the published [12]. The vibrational frequency located at 574 cm<sup>-1</sup> is the characteristic of Mn–O stretching modes in tetrahedral sites. The bands at 486 and 513 cm<sup>-1</sup> corresponds to the distortion vibration of Mn-O in an octahedra framework [13]. A small band at 3420 cm<sup>-1</sup> is caused by the stretching vibrations of the OH bond and other weak band at 1631 cm<sup>-1</sup> due to the bending vibrations of OH molecules. The peak at 1021cm<sup>-1</sup> is attributed to the OH bending modes to  $\gamma$ -OH. The FT-IR spectrum confirms the crystal structure of the sample and shows the existence of crystallization water in the sample which is necessary for battery activity [14].



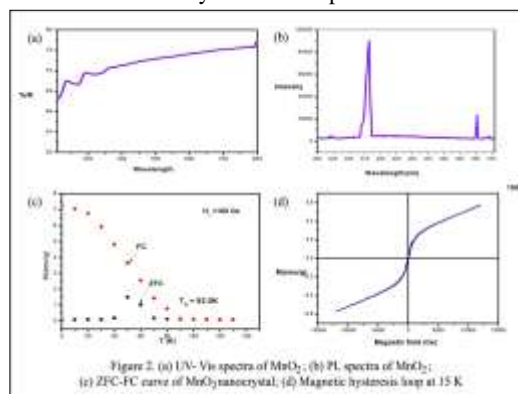
The Raman spectrum of  $\beta$ -MnO<sub>2</sub> nanopowder in figure 1c has three bands at 629, 538 and 498 cm<sup>-1</sup> which agrees well with the previous reports on the  $\beta$ -MnO<sub>2</sub> phase [15]. The Raman band at 629 cm<sup>-1</sup> is attributed to the B<sub>2g</sub> mode and involves antisymmetric Mn–O vibrations. The Raman band at 538 cm<sup>-1</sup> can be assigned to the A<sub>1g</sub> mode and is indicative of a well-developed rutile-type framework. Here, the E<sub>g</sub> mode is assigned to the band at 498 cm<sup>-1</sup>. The Raman scattering band assignment is consistent with those reported for rutile type compounds [16]. The peaks at 1824 cm<sup>-1</sup> and 1168 cm<sup>-1</sup> is ascribed to stretching and bending vibrations of the OH group [17].

SEM micrograph shown in figure 1d reveals the overall appearance of the combustion derived product. The particles are nearly spherical in shape has uniform size and distribution with varying sizes and indicates the agglomeration of nanoparticles [18].

Figure 2a shows the UV- Vis spectra of MnO<sub>2</sub>. It is found that most molecules consists of few humps rather than sharp lines which shows that the molecule is absorbing radiation over a band of wavelengths. This is due to an electronic level transition is usually accompanied by a simultaneous change between the numerous vibrational levels. The band gap energy of the as prepared sample is E<sub>g</sub>=3.185 eV [19].

PL spectra were measured for the sample in the range of 300-800nm is shown in figure 2b. The sample was excited at 360 nm, two sharp peaks at 380nm and 552nm observed in the emission spectrum. This indicates that MnO<sub>2</sub> nanopowder has a prominent blue emission peak at 380nm as well as a weak green emission at 553nm [20]. The bandgap energy was about 3.45eV.

The figure 2c shows the temperature dependence on magnetization of  $\beta$ -MnO<sub>2</sub> sample in the zero-field cooling (ZFC) and field cooling (FC) procedures. The magnetic moment is enhanced below 100K which can be confirmed by the deviation from the linear behaviour of the M against T curve. MnO<sub>2</sub> has been reported as an antiferromagnetic material with a Neel temperature, T<sub>N</sub> of 92K. Both the ZFC and FC loops deviate from antiferromagnetism under magnetic field, showing high remanent magnetism and a strong coercive field. Bulk  $\beta$ -MnO<sub>2</sub> undergoes a transition to AFM state at T<sub>N</sub> ≈ 92.5 K that exhibits both long and short range magnetic order [21]. Figure 2d shows the hysteresis loop of the  $\beta$ -MnO<sub>2</sub> nanoparticle at 15K. The hysteresis loops are not saturated under ±20k Oe due to the contribution of the antiferromagnetic core which is a common phenomenon in nanocrystalline oxide materials. The hysteresis loop shows a maximum



symmetric magnetization, M<sub>max</sub> at 0.57093 emu/g and remanence value is estimated to be 14.339 emu/g with a remanence ratio of 0.2511. The coercivity H<sub>C</sub> of the synthesized nanoparticle was 50.21Oe.

### 4. CONCLUSION

In this paper, a simple auto igniting combustion method has been successfully used to prepare  $\beta$ -MnO<sub>2</sub> nanoparticles, which are indexed as tetragonal rutile pyrolusite. As synthesized MnO<sub>2</sub> nanoparticle have been identified using XRD analysis which were proven to be single crystal in nature with an average particle size of 23 nm. The structural and functional studies were carried out using FT-IR and FT- Raman techniques. FT-IR

analysis showed a vibrational frequency as the characteristics of Mn-O stretching vibration in the tetrahedral site. The other two characteristic peak corresponds to the distortion vibration of Mn-O in an octahedral framework confirming the rutile  $\beta$ -MnO<sub>2</sub>. FT-Raman analysis revealed the characteristic peak with Mn-O vibration of the rutile type compound. The photoluminescence study showed two emission lines in the blue and green region. The UV-Vis analysis showed vibrational level transitions and some electronic states. The band gap obtained from PL and UV-Vis was found to be in the range 3.185eV – 3.45eV. The magnetic measurements revealed a Neel temperature T<sub>N</sub> of 92.5K at 100e above which the material behaves as antiferromagnetic. The remanent magnetization and coercivity was found to be 14.339 emu/g and 50.21Oe respectively.

## 5 ACKNOWLEDGMENTS

We are thankful to the Department of Physics, Karunya University Coimbatore and Electronic Materials Research Laboratory, Mar Ivanios College for their experimental facilities.

## 6. REFERENCES

- [1] C. Burda, X. Chen, R. Narayanan and M.A. El- Sayed, Chem. Rev. 105, 2005, 1025-102.
- [2] Y. Sun and Y. Xia, Science 298, 2002, 2176-179.
- [3] C.N.R. Rao, G.U. Kulkarni, P.J. Thomas and P.P. Edwards, Chem. Eur. J. 8, 2002, 28-35.
- [4] M. Sastry, Current Science 78, 2000, 1089-097.
- [5] R.N. De Guzman, Y.F. Shen, E.J. Neth, Chem. Mater. 6(6) (1994) 815–821.
- [6] X. Wang, Y.D. Li, Chem. Eur. J. 9(1) (2003) 300–306.
- [7] F. Zhou, H.G. Zheng, X.M. Zhao, Nanotechnology, 16 (2005) 2072–2076.
- [8] J.K. Yuan, W.N. Li, S. Gomez, J. Am. Chem. Soc. 127(41) (2005) 14184–14185.
- [9] D.S. Zheng, S.X. Sun, W.L. Fan, J. Phys. Chem. B. 109(34) (2005) 16439–16443.
- [10] J. Koshy, J.K. Thomas, J. Kurian, Y.P. Yadav, A.D. Damodaran, US patent. 5 (1999) 5856276.
- [11] B. Tang, G.L. Wang, L.H. Zhuo, Nanotechnology, 17(4) (2006) 947–951.
- [12] F.Y. Cheng, J. Chen, X.L. Gou, Adv. Mater. 17(2) (2005) 2753–2756.
- [13] Y.S. Ding, X.F. Shen, S. Gomez, Adv. Funct. Mater. 16 (2006) 549–555.
- [14] W.N. Li, J.K. Yuan, S. Gomez-Mower, J. Phys. Chem. B. 110(7) (2006) 3066–3070.
- [15] W.N. Li, J.K. Yuan, X.F. Shen, Adv. Funct. Mater. 16 (2006) 1247–1253.
- [16] H. Wang, Z. Lu, D. Qian, Nanotechnology. 18(11) (2007) 115616–115621.
- [18] H.E. Wang, D. Qian, Mater. Chem. Phys. 109 (2008) 399–403.
- [19] T. Shimizu, H. Asan, M. Matsui, J. Magn. Soc.Jpn, 30 (2006) 166.
- [20] D. Bahadur, J. Giri, Sadhana 28 (2003) 639-656.
- [21] L. Croguennec, P. Deniard, R. Brec, A. Lecerf, J. Mater. Chem. 5 (1995) 1919.